Optical Properties of Gold Nanoparticles: Shape and Size Effects

Parisa Khajegi and Majid Rashidi-Huyeh*

Department of Physics, University of Sistan and Baluchestan, Zahedan, Iran

***Corresponding author email:** majid.rashidi@phys.usb.ac.ir

Regular paper: Received: Mar. 6, 2021, Revised: Jun. 10, 2021, Accepted: Aug. 25, 2021,
Available Online: Aug. 27, 2021, DOI: 10.52547/ijop.15.1.41

ABSTRACT— Nobel metal nanoparticles (NPs) are widely used in various applications including optical and biological sensors, biomedicine, photocatalysts, electronics, and photovoltaic cells. The optical properties of gold NPs are surveyed in this paper under the Localized Surface Plasmon Resonance (LSPR) effect, which increases the light absorption and scattering at the LSPR wavelength. This LSPR frequency depends on various factors, including the shape and size of the particles as well as incident electromagnetic polarization. Here, the optical response of gold NPs with different shapes and sizes are investigated using the finite element method (FEM). The results show that the bandwidth, amplitude, and LSPR wavelength depend on the shape and dimensions of the NPs as well as the polarization of the incident light. The LSPR wavelength changes from 500 to 650 nm for different shapes of the gold NPs including sphere, octahedral, cube, ellipsoid, triangle, and with identical volume. To study the NP size effect on the optical properties, the absorption and scattering cross-sections (CSs) are also investigated for different sizes of NPs. The results show a redshift in the LSPR wavelength by increasing the NP size.

KEYWORDS: Absorption Cross Section, Gold Nanoparticles, Localized Surface Plasmon Resonance, Scattering Cross Section, Shape Effect.

I. INTRODUCTION

As the dimensions of the materials reduce to the nanometer scale, their physical and chemical properties change. The optical properties of the noble metal NPs are dominated by the Localized Surface Plasmon Resonance (LSPR) phenomenon. This phenomenon is related to the collective oscillation of free electrons of the metal NPs under the electromagnetic waves (EMWs) excitation. Indeed, when a metal NP is exposed by an EMW, a charge distribution may be created on the interface of the NP and the dielectric medium due to the dielectric confinement. Therefore, the oscillating electric and magnetic dipoles/multipoles can be induced [1]. When the incident EMW frequency is matched to this oscillation, a resonance may occur, known as surface plasmon resonance (SPR). By contrary to an infinite metal-dielectric interface, such as a metal layer, these surface plasmons cannot be propagated at the interface. So, they are known as localized surface plasmon resonances.

This phenomenon results in an absorption pick in a wavelength, so called the SPR wavelength. These NPs, therefore, are proposed in a wide range of medical and photonics device applications. In particular, they are proposed for enhancing the efficiency of solar cells [2], the response of surface-enhanced raman spectroscopy (SERS) [3], medical imaging, drug delivery, and cancer thermal treatment [4]-[6]. In these applications, adjustment and control of the LSPR wavelength are crucial.

The optical properties of metal NPs depend on the structure, composition, and morphology of the NPs. Such effects have been studied, experimentally as well as theoretically, by different groups [7]-[9]. In these works, absorption and/or extinction coefficient were reported for different shapes of NPs. Many

researchers have already focused on synthesize of noble metal NPs with various shapes. Different methods are also proposed for this purpose, leading to synthesizing of NPs with diverse shapes including sphere [10]-[13], ellipsoid and rod [14]-[17], triangular prisms [18]-[21], octahedral [22]-[26], and cube [27], [28]. The absorption or extinction spectra are reported in these works. From a theoretical point of view, the effects of the size or shape on the optical properties of NPs have been studied by many authors. These works are treaded by using the Mie and Gans theory [29], [30] the discrete dipole approximation [31], the finite difference time domain methods [32], and the boundary element method [33].

In this paper, we investigate the effects of the incident EMW polarization on optical properties of NPs with different shapes and sizes using the finite element method (FEM). This is especially crucial for non-spherical NPs. Moreover, the absorption and scattering cross-section (CS) profiles are determined for various shapes of NP with identical volume, including the sphere, rod, prolate ellipsoid, equilateral triangular prism, octahedral, and rectangular cube. In addition, the impact of size is also discussed on the absorption and scattering CSs for different shapes of gold NPs.

II. Model

The finite element method is used to model the optical properties of NP suspended in a dielectric medium. A scattering calculation is used, instead of the full field calculation, wherein a background field with a specific polarization is applied as the source to excite the particle. The model calculates the Helmholtz equations for EMWs and the results are obtained using a perfectly matched layer (PML) as an absorber layer in the outer domain of the modeling environment. The thickness of the PML must be at least equal to half of the EMW wavelength in the dielectric media ($\lambda_0/2n$, where n is the dielectric refractive index). The same distance of $\lambda_0/2n$ must be considered between the PML and the NP. The scattering boundary condition is used at the outer boundaries of the PML to ensure that the light cannot be reflected back to the modeling domain. The absorption and the scattering CSs are obtained from equations (1).

$$CS_{abs/scat} = \frac{W_{abs/scat}}{\frac{1}{2}\sqrt{\frac{\varepsilon}{\mu}}\left|E_{e0}\right|^2}, \tag{1}$$

where,

$$W_{abs} = \frac{1}{2}\int_{\Omega} \mathbf{J}\cdot\mathbf{E}dv, \tag{2}$$

$$W_{scat} = \int_{S_c} \mathbf{n}\cdot\langle\mathbf{S}_{scat}\rangle dS = \frac{1}{2}\int_{S_c} \mathbf{n}\cdot\mathrm{Re}\left\{\mathbf{E}_s\times\mathbf{H}_s^*\right\}dS \tag{3}$$

are absorbed power in the NP and scattered power, respectively. The integration of absorbed and scattered power are performed on the overall volume of the particle of Ω and on the particle surface of S_c. **J**, **E**, **H**, **S**, and **n** represent current density, electric field, magnetic field, Poynting's vector, and the particle surface normal vector respectively [34]. The model is first validated by comparing the results with those obtained using Mie theory [35] for two small and large nanospheres with radii of 10 and 100 nm. The results are shown in Fig. 1, which presents the normalized absorption CSs. As seen, the simulation results have shown a very good agreement with those obtained by Mie theory.

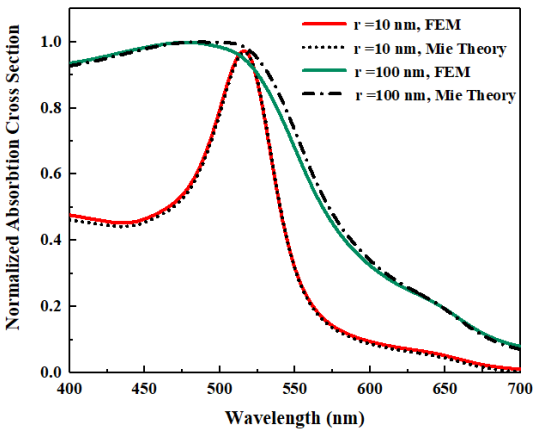

Fig. 1. Comparing the results obtained using simulation by FEM method with those calculated by using Mie theory for the small and large spherical

nanoparticle with radii of 10 and 100 nm suspended in the water with the refractive index of 1.34.

To study the NP shape and size effect on the optical properties, different shapes of sphere, ellipsoid, octahedral, rectangular cubic, equilateral triangular prism, and rod NPs with different sizes are considered. The NPs dimensions were chosen so that their volume remains constant, corresponding to a sphere with a radius of 10 nm. The NPs dimensions are summarized in table 1.

Table **1** Geometrical properties of simulated gold nanoparticles

Geometry	Dimension (nm)
Sphere	r=10
Rod	D=12, L=36
Prolate Ellipsoid	a=b=8, c=16
Rectangular Cube	Side Length=19, Height=10
Equilateral Triangular prism	Side Length=30, Height=10
Octahedral	Side Length=20

The air is considered as the surrounding medium. Moreover, in each NP shape, the incident light polarization was chosen so that maximum SPR amplitude could be achieved. For instance, Fig. 2 represents the absorption CSs of equilateral triangular NP with different incident light polarizations. The maximum LSPR amplitude is corresponding to the z propagation of EMW with polarization in x and y directions.

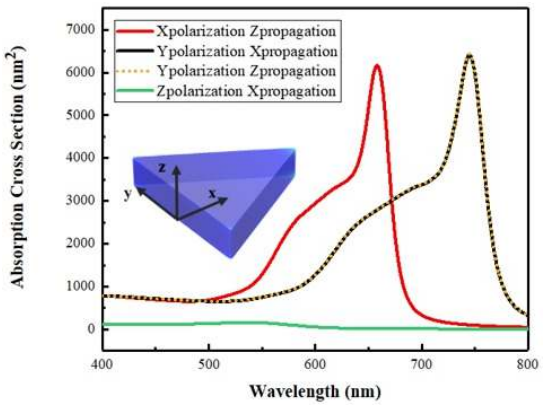

Fig. 2. Absorption CS of an equilateral triangular NP with a side length of 50 nm and height of 10 nm for three different polarizations and propagation directions of incident EMW.

III. Results And Discussion

A. *Shape Effect*

To investigate the shape effect of NPs on the optical properties, the absorption and scattering CSs are compared for different shapes of spherical, elliptical, cubic, rod, octahedral and triangular NPs. As mentioned, for non-spherical NPs, in which the intensity of absorption depends on the incident light polarization, the polarization with the highest absorption intensity is considered. The results are shown in Fig. 3. The LSPR wavelength for spherical, octahedral, elliptical, cubic, triangular, and rod NPs are located at 502, 520, 526, 532, 562, and 634 nm, respectively (see inset in Fig. 3(a). For triangular prism and octahedral NPs, a shoulder shape may be observed in the absorption CS spectra. This shoulder is located in a wavelength that is larger than that the LSPR wavelength. The LSPR bandwidth and amplitude depend also on the particle shape. While the maximum amplitude is observed for the nanorod, the lowest one is for the spherical NP. The peak in the nanorod is related to the longitudinal mode, which is caused by electrons oscillation along its longer dimension. To understand these behaviors, let us first mention that as the sizes of nanoparticles are very smaller than the incident light wavelength, the NPs optical responses may be given by dipole approximation very well. Under an EMW excitation, the negative and positive charges separate from each other. So, an electric dipole moment is induced. The longer is the particle, the stronger is the electric dipole moment. Thus, by increasing the length of the particle, the LSPR wavelength presents a redshift and the LSPR amplitude increases. By increasing the particle edge number, its optical properties get closer to sphere ones. This behavior can be seen in Fig. 3(a), by comparing the LSPR wavelength of cubic, octahedral, and spherical nanoparticles.

On the other hand, the LSPR edge modes are determining for NPs with sharp edges. This is related to the enhancement of the electric field due to the surface electric charge density, and is shown in Fig. 4, in which the electric field intensity is exhibited for different NP shapes at

LSPR wavelength. Fig. 3(b). represents the scattering CS for the same NPs. It should be noted that scattering CS values are lower than the absorption ones for the considered particle size. The maximum value for octahedral, cubic, spherical, elliptical, triangular, and rod NPs are located at 526, 532, 544, 556, 556, and 628 nm, respectively. For NPs containing the edges and vertices, such as triangular and octahedral, a second peak (or shoulder) are seen, which are related to the edge mode (see inset in Fig. 3(b)).

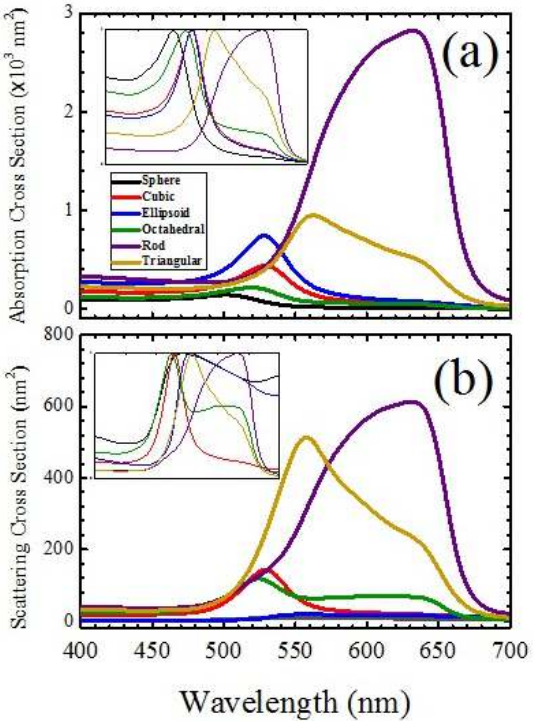

Fig. 3. Absorption (a) and Scattering (b) CSs for different particle shapes, presented in table 1. The insets show the normalized spectra.

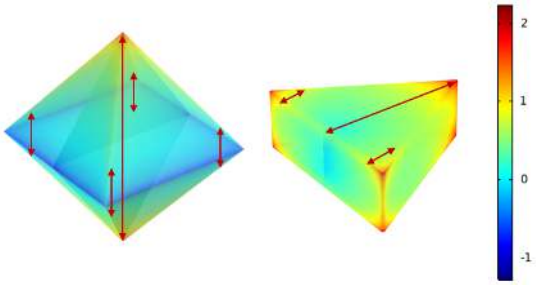

Fig. 4. Electric field norm profile in logarithm scale at LSPR wavelength (520 nm for octahedral and 562 nm for triangular prism). The arrows show the incident EMW polarization.

B. *Size Effect*

To study the NPs size effects on the optical properties, the absorption and scattering CSs per particle volume are calculated for spherical, rod, and triangular prism NPs with different sizes. The results for spherical NPs with radii of 10 to 100nm are depicted in Fig. 5. By increasing the NP size, the amplitude of absorption CS per particle volume increases and, then it decreases. On the other hand, by increasing the NP size, the absorption CS bandwidth increases, and a weak redshift is observed in the LSPR wavelength. In fact, for the tiny particles with a dimension very smaller than the incident electromagnetic wavelength, just electric dipole may be excited, but for the particles with sizes comparable to the incident EMW, the electric multipolar can be excited.

Also, with increasing the NPs size the electric dipoles moment power increase [36], [37]. So, the absorption CSs are enhanced, and the LSPR wavelengths displace to longer wavelengths (a redshift displacement). On the other hand, by evident, with increasing the particle size, its volume increases, and therefore absorption CS per volume particle decreases. These two contradictory size effects can very well explain the behaviors of the absorption CS per particle volume. The same behaviors may be observed in the scattering CS for the Spherical NPs (see Fig. 5b). Indeed, for the NPs with dimensions very smaller than the incident EMW, the scattering CS is negligible, but by increasing the NP size, it increases gradually, because of the increasing the electric dipole power on one hand, and the creation of the electric multipole effects, on the other hand.

As there was mentioned, the longitudinal and edge LSPR modes are determining for rod and triangular prism NPs, respectively. Now, it is interesting to study the size effects of these NPs on their optical properties. To this end, the absorption and scattering CSs per NP volume are determined for the rod with 12 and 36 nm of diameter and an aspect ratio (L/D) of 3, and the equilateral triangular prism with the sides of 30 and 90 nm and the height of 10 nm.

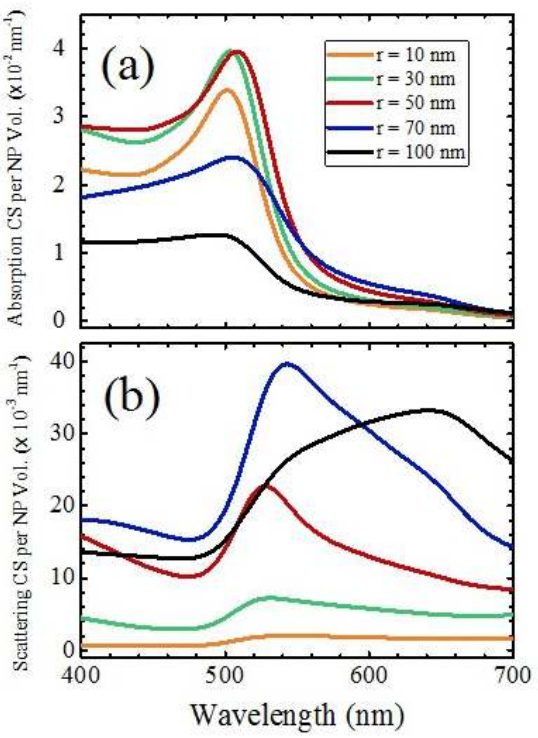

Fig. 5. Absorption (a) and Scattering (b) CS per NP volume for gold spherical NPs by different radii of 10, 30, 50, 70, and 100 nm.

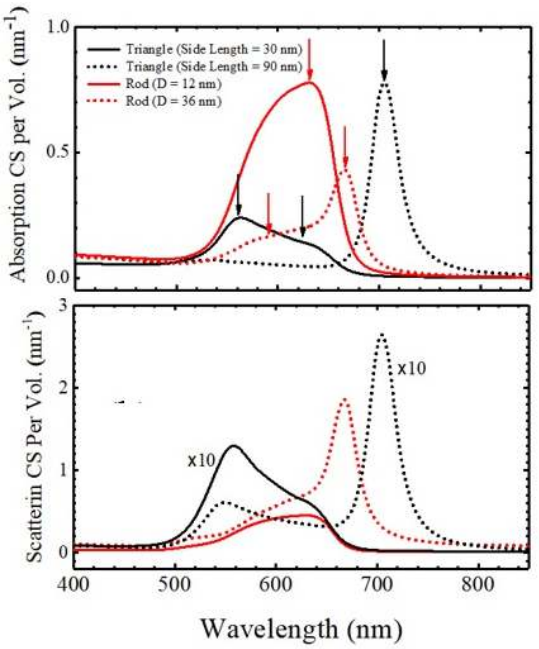

Fig. 6. Absorption (a) and Scattering (b) CS per NP volume for a rod with diameters of 12 and 36 nm and an aspect ratio (L/D) of 3, and the equilateral triangular prism with a sides of 30 and 90 nm and the height of 10nm. The values of scattering CS of triangular NP are magnified by a factor of 10 for better visibility.

By increasing the nanorod size, LSPR wavelength presents a redshift displacement and a second LSPR mode appears in the absorption and scattering CSs per particle volume, located in the shorter wavelength. Moreover, the amplitude of absorption CS per NP volume decreases. In the triangular NP case, by increasing the length side, LSPR wavelength experiences a redshift, same as the nanorod case, but contrary to the nanorod, the amplitude absorption CS per NP volume increases. In the two cases of nanorod and triangular prism, by increasing the particle size, the scattering CS per NP volume increase (Fig. 6b). These behaviors are related to the stronger electric dipole moment and appearance of the electric multipoles for the larger particle size. It is also noteworthy to mention that the electric multipole is more effective in the nanorod comparing with the triangular prism NPs, because of the considered morphology.

IV. Conclusion

In this paper, the shape and size effects of gold NPs on their optical properties were studied. Different NPs shapes were considered, including the sphere, rod, ellipsoid, octahedral, cube, and equilateral triangular prism. The results showed that the shape of the NPs affect the LSPR wavelength and amplitude. For the elongate particles such as rod and prolate ellipsoid NPs, longitudinal LSPR mode is governed on their optical properties, while in the NPs possessing the edges in their geometry, same as cubic, octahedral, and triangular NPs, the LSPR edge mode plays a crucial role. These results can help in many applications such as the design and fabrication of photonic devices, solar cells, and medical area. In such applications, one may need absorption and/or scattering CSs.

References

[1] W. Krasser and J. Tiggesbaumker, *Uwe Kreibig and Michael Vollmer: Optical Properties of Metal Clusters,* Springer Verlag, Berlin, 1995.

[2] S. Castelletto and A. Boretti, "Noble metal nanoparticles in thin film solar cells,"

Nanosci. Nanotechnol. Lett. Vol. 5, pp. 36-40, 2013.

[3] L.L. Tan, M. Wei, L. Shang, and Y.W. Yang, "Cucurbiturils-Mediated Noble Metal Nanoparticles for Applications in Sensing, SERS, Theranostics, and Catalysis," Adv. Funct. Mater. Vol. 31, pp. 2007277 (1-26), 2021.

[4] M. Sharifi, F. Attar, A.A. Saboury, K. Akhtari, N. Hooshmand, A. Hasan, M.A. El-Sayed, and M. Falahati, "Plasmonic gold nanoparticles: Optical manipulation, imaging, drug delivery and therapy," J. Control. Release, Vol. 311, pp. 170-189, 2019.

[5] H. Kang, J.T. Buchman, R.S. Rodriguez, H.L. Ring, J. He, K.C. Bantz, and C.L. Haynes, "Stabilization of silver and gold nanoparticles: preservation and improvement of plasmonic functionalities," Chem. Rev. Vol. 119, pp. 664-699, 2018.

[6] X. Huang and M.A. El-Sayed, "Gold nanoparticles: Optical properties and implementations in cancer diagnosis and photothermal therapy," J. Adv. Res. Vol. 1, pp. 13-28, 2010.

[7] R.D. Averitt, S.L. Westcott, and N.J. Halas, "Linear optical properties of gold nanoshells," J. Opt. Soc. Amer. B, Vol. 16, pp. 1824-1832, 1999.

[8] R. Rodríguez-Oliveros and J.A. Sánchez-Gil, "Gold nanostars as thermoplasmonic nanoparticles for optical heating," Opt. Express, Vol. 20, pp. 621-626, 2012.

[9] G.S. He, J. Zhu, K.-T. Yong, A. Baev, H.-X. Cai, R. Hu, Y. Cui, X.-H. Zhang, and P. Prasad, "Scattering and absorption cross-section spectral measurements of gold nanorods in water," J. Phys. Chem. C, Vol. 114, pp. 2853-2860, 2010.

[10] L. M. Liz-Marzán, "Tailoring surface plasmons through the morphology and assembly of metal nanoparticles," Langmuir, Vol. 22, pp. 32-41, 2006.

[11] P.N. Njoki, I.-I.S. Lim, D. Mott, H.-Y. Park, B. Khan, S. Mishra, R. Sujakumar, J. Luo, and C.-J. Zhong, "Size correlation of optical and spectroscopic properties for gold nanoparticles," J. Phys. Chem. C, Vol. 111, pp. 14664-14669, 2007.

[12] V. Amendola and M. Meneghetti, "Laser ablation synthesis in solution and size manipulation of noble metal nanoparticles," Phys. Chem. Chem. Phys. Vol. 11, pp. 3805-3821, 2009.

[13] S. Hashemizadeh and M. Rashidi Huyeh, "Silver nanocolloid: synthesis, optical and thermo-optical properties," Sci. Adv. Mater. Vol. 829, pp. 670-674, 2014.

[14] C.J. Murphy, T.K. Sau, A.M. Gole, C.J. Orendorff, J. Gao, L. Gou, S.E. Hunyadi, and T. Li, "Anisotropic metal nanoparticles: synthesis, assembly, and optical applications," J. Phys. Chem. B, Vol. 109, pp. 13857-13870, 2005.

[15] J. Cao, T. Sun, and K.T. Grattan, "Gold nanorod-based localized surface plasmon resonance biosensors: A review," Sens. Actuator B-Chem.Vol. 195, pp. 332-351, 2014.

[16] L. Scarabelli, C. Hamon, and L.M. Liz-Marzán, "Design and fabrication of plasmonic nanomaterials based on gold nanorod supercrystals," Colloidal Synthesis Plasmonic Nanometals, Vol. 29, pp. 677-706, 2020.

[17] Z.-C. Xu, C.-M. Shen, C.-W. Xiao, T.-Z. Yang, S.-T. Chen, H.-L. Li, and H.-J. Gao, "Fabrication of gold nanorod self-assemblies from rod and sphere mixtures via shape self-selective behavior," Chem. Phys. Lett. Vol. 432, pp. 222-225, 2006.

[18] J. E. Millstone, G.S. Métraux, and C.A. Mirkin, "Controlling the edge length of gold nanoprisms via a seed-mediated approach," Adv. Funct. Mater. Vol. 16, pp. 1209-1214, 2006.

[19] A. Miranda, E. Malheiro, E. Skiba, P. Quaresma, P.A. Carvalho, P. Eaton, B. de Castro, J.A. Shelnutt, and E. Pereira, "One-pot synthesis of triangular gold nanoplates allowing broad and fine tuning of edge length," Nanoscale, Vol. 2, pp. 2209-2216, 2010.

[20] M. Klekotko, J. Olesiak-Banska, and K. Matczyszyn, "Photothermal stability of biologically and chemically synthesized gold nanoprisms," J. Nanoparticle Res. Vol. 19, pp. 1-9, 2017.

[21] C. Xue, Z. Li, and C.A. Mirkin, "Large-Scale Assembly of Single-Crystal Silver Nanoprism Monolayers," Small, Vol. 1, pp. 513-516, 2005.

[22] C. Li, K.L. Shuford, Q.H. Park, W. Cai, Y. Li, E.J. Lee, and S.O. Cho, "High-yield synthesis of single-crystalline gold nano-octahedra," Angew. Chem. Vol. 119, pp. 3328-3332, 2007.

[23] C. Cao, S. Park, and S.J. Sim, "Seedless synthesis of octahedral gold nanoparticles in condensed surfactant phase," J. Colloid Interface Sci. Vol. 322, pp. 152-157, 2008.

[24] C.C. Chang, H.L. Wu, C.H. Kuo, and M.H. Huang, "Hydrothermal synthesis of monodispersed octahedral gold nanocrystals with five different size ranges and their self-assembled structures," Chem. Mater. Vol. 20, pp. 7570-7574, 2008.

[25] P.J. Chung, L.M. Lyu, and M.H. Huang, "Seed-Mediated and Iodide-Assisted Synthesis of Gold Nanocrystals with Systematic Shape Evolution from Rhombic Dodecahedral to Octahedral Structures," Chem. Eur. J. Vol. 17, pp. 9746-9752, 2011.

[26] Y. Chen, X. Gu, C.-G. Nie, Z.-Y. Jiang, Z.-X. Xie, and C.-J. Lin, "Shape controlled growth of gold nanoparticles by a solution synthesis," Commun. Chem. Vol. 33, pp. 4181-4183, 2005.

[27] X. Lu, M. Rycenga, S.E. Skrabalak, B. Wiley, and Y. Xia, "Chemical synthesis of novel plasmonic nanoparticles," Annu. Rev. Phys. Chem. Vol. 60, pp. 167-192, 2009.

[28] J. Krajczewski, M. Kędziora, K. Kołątaj, and A. Kudelski, "Improved synthesis of concave cubic gold nanoparticles and their applications for Raman analysis of surfaces," RSC adv. Vol. 9, pp. 18609-18618, 2019.

[29] S. Link, M. Mohamed, and M. El-Sayed, "Simulation of the optical absorption spectra of gold nanorods as a function of their aspect ratio and the effect of the medium dielectric constant," J. Phys. Chem. B, Vol. 103, pp. 3073-3077, 1999.

[30] P. K. Jain, K.S. Lee, I.H. El-Sayed, and M.A. El-Sayed, "Calculated absorption and scattering properties of gold nanoparticles of different size, shape, and composition: applications in biological imaging and biomedicine," J. Phys. Chem. B, Vol. 110, pp. 7238-7248, 2006.

[31] T. Jensen, L. Kelly, A. Lazarides, and G.C. Schatz, "Electrodynamics of noble metal nanoparticles and nanoparticle clusters," J. Clust. Sci. Vol. 10, pp. 295-317, 1999.

[32] P. Das, T.K. Chini, and J. Pond, "Probing higher order surface plasmon modes on individual truncated tetrahedral gold nanoparticle using cathodoluminescence imaging and spectroscopy combined with FDTD simulations," J. Phys. Chem. C, Vol. 116, pp. 15610-15619, 2012.

[33] L. Bonatti, G. Gil, T. Giovannini, S. Corni, and C. Cappelli, "Plasmonic Resonances of Metal Nanoparticles: Atomistic vs. Continuum Approaches," Front. Chem. Vol. 8, pp. 340 (1-15), 2020.

[34] A. Doicu, T. Wriedt, and Y.A. Eremin, *Light scattering by systems of particles: null-field method with discrete sources: theory and programs*, Springer, 2006.

[35] G. Mie, "Articles on the optical characteristics of turbid tubes, especially colloidal metal solutions," Ann. Phys. Vol. 25, pp. 377-445, 1908.

[36] J.Y. Yan, W. Zhang, S. Duan, X.-G. Zhao, and A.O. Govorov, "Optical properties of coupled metal-semiconductor and metal-molecule nanocrystal complexes: Role of multipole effects," Phys. Rev. B, Vol. 77, pp. 165301 (1-9), 2008.

[37] J.Z. Zhang, *Optical properties and spectroscopy of nanomaterials,* World Scientific, 2nd Ed, 2009.

Parisa Khajegi received the B.Sc. degree in physics from Birjand University, Birjand, Iran, in 2012, the M.Sc. degree in photonics from Sistan and Baluchestan University, Zahedan, Iran, in 2015. Currently, she pursues again M.Sc. degree in plasma physics at Shahid Beheshti University, Tehran, Iran.

Majid Rashidi-Huyeh received the B.Sc. degree in applied physics from Ferdowsi

University of Mashhad (FUM), Mashhad, Iran, in 1994, the M.Sc. degree in atomic physics from the Institute for Advanced Studies in Basic Sciences (IASBS), Zandjan, Iran, in 1997, and the Ph.D degree in solid particles physics from Institute of Nano-Science of Paris (INSP) in University of Pierre and Marie Curie (UPMC), Paris, France, in 2006. He joined the University of Sistan and Baluchestan, Department of Physics, in 1997. He is, currently, an associate professor at the University of Sistan and Baluchestan. His works are focused on the optical and thermo-optical properties of the nanostructures.